Optimized design methodology in inductive power transfer systems applied to electric vehicle charging

Leonardo A. Brum Viera[1], Pedro Gelati Pascoal[2], Cassiano Rech[1]
[1] *Federal Universtity of Santa Maria (UFSM), Santa Maria - RS, Brazil*
[2] *INESC TEC - Institute of Systems and Computer Engineering, Technology and Science, Porto - Portugal*
leonardo.viera@ufsm.acad.br, pedropascoal01@hotmail.com, cassiano.rech@ufsm.br.

***Abstract*—Technologies related to the transportation electrification have been gaining attention in recent years. One technology that stands out is wireless charging, which still presents numerous challenges in terms of design and optimization of parameters. This article proposes a design methodology for optimizing the performance of an inductive power transfer (IPT) for wireless charging of electric vehicles, taking into account operating limits. The proposed methodology uses a PSO (Particle Swarm Optimization) algorithm to find the design variables that maximize the eficiency. The methodology and the development of a 3.6 kW experimental setup are presented, resulting in a power transfer efficiency of 89.4 %.**

***Index Terms*—Wireless Power Transfer (WPT), Inductive Power Transfer (IPT), Electric Vehicle, Wireless Charger, Optimization Design, Particle Swarm Optimization (PSO).**

I. Introduction

Over the past century, societal development has become closely tied to the extraction and consumption of fossil energy. One of the primary issues associated with fossil fuels is the ongoing increase in environmental pollution and its adverse effects on human health.The economic sector with the highest demand for fossil energy is the transportation sector, responsible for consuming 60% of the total amount of oil produced [1]. Considering this, electric vehicles (EVs) emerge as an alternative for urban mobility and have the potential to reduce the consumption of fossil fuels and their adverse effects [2].

An estimate of the electric vehicle (EV) fleet conducted by the IEA shows a significant increase in EVs from 2015 to 2021, with an exponential growth trend. EV sales doubled in 2021 compared to the previous year, accounting for 10% of total vehicle sales. The surge in EV sales can be attributed to several key factors, including political support, an increasing number of countries committing to gradually phase out internal combustion engines, and initiatives from automakers to electrify their fleets in addition to the defined policy goals [1]. Brazil is also experiencing an increase in EV adoption, reflecting the rising interest in sustainable mobility [3], [4].

However, EVs demonstrate limitations related to batteries, which have unsatisfactory energy density, providing considerably low autonomy compared to combustion vehicles. In addition, batteries still have a limited lifespan and high cost. Therefore, one of the main challenges of electrically powered urban transportation is related to their charge accumulators, as well as charging methods.

Identify applicable funding agency here. If none, delete this.

These trends highlight the importance of continuous advancements in technology to further drive the transition to electric vehicles. One innovative technology in this field is the Wireless Power Transfer (WPT) charging system. The WPT enables convenient and efficient charging of EVs without the need for physical cables, offering greater convenience and accessibility for EV owners. Inductive Power Transfer (IPT), one of the WPT technologies, is extensively used in electric vehicle charging applications.

When designing IPT systems one of the main concerns is about PTE (Power Transfer Efficiency). Various methodologies can be employed to maximize its efficiency, even for load variations and misalignment operation. An optimization technique is presented in [5], using multiple trasmitting coils and an adaptive control to select the coil most aligned with the vehicle to maximize PTE. In [6], a 2-D finite-element analysis (FEA) to determine the optimum design parameters of the system coils is presented, comparing misalignment and coils cost.

In all these techniques, the design starts with the geometry of the coils and then the components are chosen based on the magnitudes of the electrical variables. In this way, it becomes interesting to design the IPT system taking into account the current and voltage limits in the circuit to suit the available components. Therefore, this article introduces a novel approach to enhance the efficiency of Inductive Power Transfer (IPT) systems through the optimization of design variables using the PSO algorithm taking boundary conditions of maximum voltage and maximum current across the components.

The IPT system operational principles are discussed, followed by a comprehensive presentation of the proposed design methodology. Experimental results are presented to validate the effectiveness of the optimization technique in achieving maximum system efficiency.

II. IPT System Description

The IPT system under study is illustrated in Figure 1. The circuit has two main parts, one external to the vehicle (transmission side) and composed of a high-frequency DC/AC full-bridge inverter, a transmission coil (L_1) and the compensation capacitance (C_1). The inverter has the function of injecting high-frequency alternating current into the transmission coil, which in turn generates an electromagnetic field. Due to the high-reluctance air core, it is necessary to insert the

compensation circuit, in this case a capacitor in series, sized to compensate the leakage inductance of the primary coil. In addition, the IPT charger has a front-end converter (usually a PFC boost converter) connected to the grid, but it is not the main focus of this work. Therefore, it was not taken into account in this analysis.

The other part of the system is internal to the vehicle (receiving side) and comprises a receiving coil (L_2), the compensation capacitor (C_2), a passive full-bridge rectifier (AC/DC) and a synchronous buck-boost converter. In this part of the circuit, the receiving coil captures the electromagnetic field produced by the primary coil, which is compensated by the series capacitor and then rectified by the passive diode bridge, generating a dc bus voltage for the buck-boost converter that interfaces with the battery.

The system is controlled in the primary and secondary sides, where the secondary buck-boost converter has the function of guaranteeing adequate voltage and current levels for battery charging, while the primary inverter uses a perturb and observe algorithm to track the maximum efficiency transmission point.

A. Series-Series Steady-State Electrical Model

The design methodology relies on the steady-state analytical equations of the circuit. Consequently, , a simplified circuit is considered for modeling. For this purpose, it is utilized a first harmonic approximation, which considers that in a resonant system the only component of the Fourier series that contributes to power transfer is the component at the fundamental frequency [7]. Through this approximation, it is possible to replace the input inverter with an alternating voltage source at the resonance frequency of the system. Furthermore, the battery, output rectification and buck-boost converter was replaced by an equivalent resistive load, representing a specific operation point. The resulting simplified circuit is illustrated in Figure 2.

In Figure 2, r_{L1}, r_{L2}, and R_{oe} represent, respectively, the resistance of the transmission coil, the resistance of the reception coil, and the equivalent load resistance of the circuit. The voltage v_{ie} represents the amplitude of the first harmonic synthesized by the inverter, considering symmetric phase-shift modulation. The relationship between the phase angle of the arms (φ) and v_{ie} can be expressed as follows

$$v_{ie} = \frac{1}{2\sin^{-1}\left(\frac{\pi\sqrt{2}}{4\varphi V_{in}}\right)}. \tag{1}$$

The equivalent output resistance (R_{oe}) can be found using the static gain of the buck-boost converter, where the resistance reflected at the converter input (R_{eq}) is expressed by

$$R_{eq} = \left(\frac{1-D}{D}\right)^2 R_o \tag{2}$$

where R_o represents the equivalente resistance of the battery determined using power and voltage measurements at a specific operating point, and D is the duty-cycle of buck-boost converter. Considering the Fundamental Harmonic approximation (FHA) [8], the equivalent R_{oe} could be express as

$$R_{oe} = \frac{8}{\pi^2} R_{eq}. \tag{3}$$

In compensation topologies, IPT can be used in two desing modes. The first involves designing the capacitors to operate in resonance with the leakage inductances, while in the second method, capacitors are sized for resonance with the self-inductances of the coils. In [9], both techniques are compared, with compensation through self-inductance showing higher efficiency and greater robustness against coil misalignment variations. Therefore, we chose to perform this analysis considering capacitors C_1 and C_2 operating in resonance with self-inductances L_1 and L_2, respectively. Thus, the capacitances of the circuit can be desing using the following equations

$$C_1 = \tfrac{1}{\omega^2 L_1} \qquad C_2, = \tfrac{1}{\omega^2 L_2} \tag{4}$$

In this way, for an operating frequency ω_0 the primary and secondary reactances are cancelled, so that:

$$1/j\omega_0 C_1 = j\omega_0 L_1 \quad , \quad 1/j\omega_0 C_2 = j\omega_0 L_2. \tag{5}$$

For the static analysis, the dynamic voltage and current components were replaced by their steady-state phasor equivalents. The phasors are the rms values of the sinusoidal voltages and currents, defined by:

$$\begin{aligned} v_{ie} &= \mathrm{V}_{ie}\sqrt{2}sin(\omega t) \\ i_1 &= \mathrm{I}_1\sqrt{2}sin(\omega t + \theta_1) \\ v_o &= \mathrm{V}_o\sqrt{2}sin(\omega t + \theta_2) \\ i_2 &= \mathrm{I}_2\sqrt{2}sin(\omega t + \theta_2) \end{aligned} \tag{6}$$

Using Kirchhoff Law it is possible to write the primary current (I_1) and secundary current (I_2) as

$$\mathrm{I}_1 = \frac{V_{ie}(r_{L2} + R_{oe})}{\omega^2 M^2 + r_{L1}(r_{L2} + R_{oe})}, \tag{7}$$

$$\mathrm{I}_2 = \frac{V_{ie}(j\omega M)}{\omega^2 M^2 + r_{L1} r_{L2} + R_{oe} r_{L1}}. \tag{8}$$

Multiplying 8 by the load resistance R_o we obtain the output voltage, represented by

$$\mathrm{V}_\mathrm{o} = \frac{V_{ie}(j\omega M) R_{oe}}{\omega^2 M^2 + r_{L1} r_{L2} + R_{oe} r_{L1}} \tag{9}$$

Multiplying (8) by the 8 by Equation 9 gives the following expression for output power

$$P_o = \frac{{V_{ie}}^2 \omega^2 M^2 R_{oe}}{\left[\omega^2 M^2 + r_{L1} r_{L2} + R_{oe} r_{L1}\right]^2}. \tag{10}$$

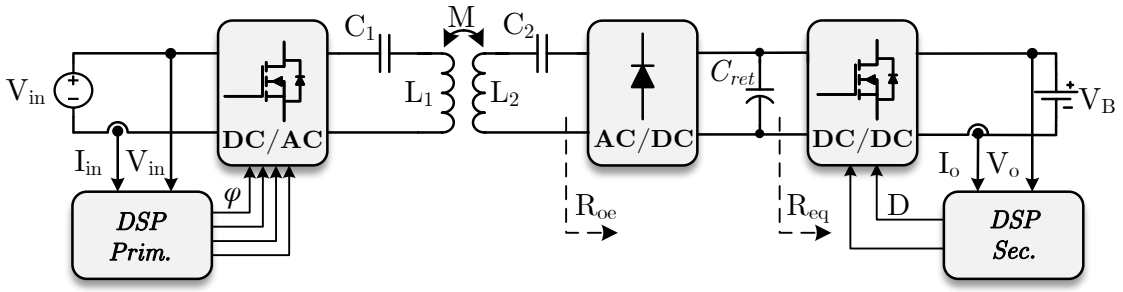

Figure 1: IPT charging system.

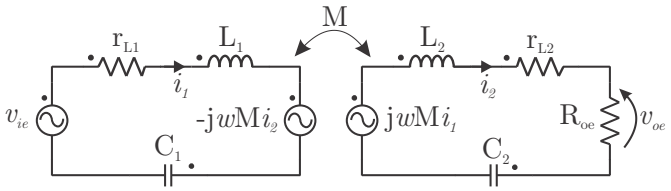

Figure 2: IPT simplified circuit.

The apparent input power is calculated by multiplying the rms value of the input voltage V_{ie} by the modulus of 7, and it can be expressed as:

$$S_{in} = \frac{{V_{ie}}^2(r_{L2} + R_{oe})}{\omega^2 M^2 + r_{L1}(r_{L2} + R_{oe})}. \tag{11}$$

The input active power can be calculated by multiplying 11 and the of the input current angle I_1. However, it is observed that 7 does not present an imaginary part due to the employed compensation method. In this way, the system does not present a phase difference between the input current and voltage, operating with unity power factor. Therefore, the input power can be given as:

$$P_{in} = \frac{{V_{ie}}^2(r_{L2} + R_{oe})}{\omega^2 M^2 + r_{L1}(r_{L2} + R_{oe})}. \tag{12}$$

Therefore, the circuit efficiency can be obtained from 10 and 12, and it can be given by:

$$\eta = \frac{R_{oe}}{\left[1 + \frac{r_{L1}(r_{L2}+R_{oe})}{\omega^2 M^2}\right](r_{L1} + r_{L2})}. \tag{13}$$

The voltage across the capacitors can be calculated using

$$V_{C1} = I_1 / j\omega_0 C_1 \tag{14}$$

$$V_{C2} = I_2 / j\omega_0 C_2. \tag{15}$$

B. Coils Design

The main indicators analyzed when designing the coils in a WPT system are the quality factor and the coupling coefficient [10]. The first is improved by reducing the conductor resistance (r_L), which is dependent on the skin effect and the proximity effect, as well as dispersion losses, and by increasing the values of self-inductance. The second is mainly dependent on the distance between the coils and their misalignment. Therefore, to achieve the desired coupling coefficient, the coil must be designed for specific distance and misalignment values [11].

Currently, the literature presents different coil configurations, such as circular, square, rectangular and three-dimensional spiral (solenoid). These projects can be considered as the basis for the formation of other arrangements, such as the DD coil, DDQ and bipolar multi-coils [11].

In [12] and [13], it was concluded that the circular coil ends up occupying less space, requiring less material, and having greater tolerance to misalignmet, resulting in better performance in terms of mutual inductance parameters, coupling coefficient, magnetic flux, and magnetic field.

Taking into account the geometry of the flat circular coil, the design variables are illustrated in Figure 3.

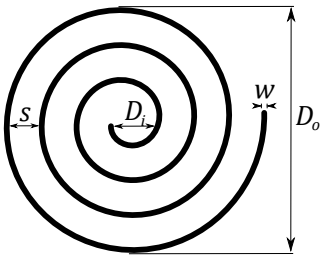

Figure 3: Parameters of the flat circular coil.

Parameters D_o and D_i are, respectively, the external and internal diameter of the coil. The section of the conducting wire is represented by w, the spacing between the turns is described as s and N symbolizes the number of turns. The self inductance of flat circular coils is established [14] by

$$L = \frac{\mu_0 N^2 (D_o + D_i)}{4}[ln\frac{2,46}{\varphi} + 0,2\varphi^2\omega], \tag{16}$$

where φ is equivalent to:

$$\varphi = \frac{(D_o - D_i)}{(D_o + D_i)} \tag{17}$$

and μ_0, represents the permeability of the vacuum,

$$\mu_0 = 4\pi.10^{-7}\ H/m. \tag{18}$$

Note that to determine the coils' self inductance, their internal diameter is necessary, which can be established according to (19):

$$D_i = D_o - (2wN) - (2s(N-1)). \tag{19}$$

To determine D_i, the section of the conductor wire, the number of windings and the spacing between the turns are essential. In this way, the design of the inductive coupling can be started by specifying the conductor wire. To achieve this, a litz wire methodology is considered [13], [15]. Through this methodology followed.Through this project it is possible to analytically estimate the final resistance of the conductor, which will directly impact the system losses, using

$$R_L = \frac{\rho l}{A_{str}}.N_{str}. \tag{20}$$

Where R_L represents the total resistance of the conductor, since AC losses are ideally eliminated using the Litz wire. N_{str} corresponds to the total number of conductors (*strands*) making up the Litz wire, A_{str} symbolizes the area of each of these conductors, ρ is the resistivity of the copper and l is the conductor length.

III. Design optimization technique

A. Design specifications

Table I shows the specifications of the IPT charger under development.

Table I: Design specifications for the IPT system

Parameter		Value
Input Voltage	V_{in}	400 V
Output Nominal Voltage	V_o	360 V
Nominal Output Power	P_o	3.6 kW
Operation Frequency	f_s	85 kHz
Coils Gap	D_{Gap}	160 mm
Nominal coupling factor	k	0.2
Compensation topology		Series-Series

The operating frequency and the distance between the coils was defined based on the SAE-J2954 standard. Since the frequency can vary between 79 kHz - 90 kHz. The definition of the distance between the coils was based on the Z2 class, which defines a nominal operation for a distance between 100 mm and 210 mm. Based on [16], it is argued that for this distance a commonly found value for the coupling factor is 0.2.

In [17], a comparison between SS (Series-Series) and SP (Series-Parallel) compensations topology is presented, and it is concluded that both are equivalent in terms of the main performance requirements and power transferred to the load. However, the SS topology has a significant advantage in that resonance is independent of both the load and the coupling factor, making it more robust for applications with misalignment [18].

B. Iterative IPT simulation algorithm

The proposed design methodology consists of using a simplified model of the system, as shown in Figure 2. Analyzing this figure, it can be seen that the circuit has four design variables, namely: input voltage amplitude (V_{ie}), the inductance L_1, the inductance L_2 and the duty cycle of the buck-boost converter (D) intrinsic to the R_{eq}. The other parameters such as series resistance of the coils (r_{L1} and r_{L2}) and compensation capacitors (C_1 and C_2) are linked to the inductance values and the physical design of the coils.

Usually in the design of resonant converters, a variable called output quality factor (Q_o) is used as a design parameter, which usually varies between 2 and 10 for IPT [19] systems and can be defined as:

$$Q_o = \frac{\omega_0 L_2}{R_{eq}} \tag{21}$$

where ω_0 is the operating frequency.

From 21, one can observe that the quality factor is dependent on both the output load resistance and the self-inductance of the secondary coil. Therefore, it is possible to define new design variables, these being the input voltage (V_{ie}), the output quality factor (Q_o), which adds the duty ratio and secondary self-inductance. And in addition to these, it is possible to define a ratio between the primary and secondary inductances (L_1/L_2) as a variable instead of a directly arbitrary value for L_1.

Based on these three design parameters, an iterative algorithm was developed, aiming to simulate the behavior of the main circuit variables when the design parameters vary. In this case, it was decided to check the behavior of the effective primary current I_{1rms}, effective secondary current I_{2rms}, peak voltage in the capacitors V_{C1pk} and V_{C2pk}, the duty ratio of the *buck-boost* converter (D) and the circuit efficiency (η).

The Newton Raphson algorithm was used to compute the variables of the system. the variables converge to the values that guarantee the power and output voltage specified in the project. As an example, the variables of interest were plotted as a function of the quality factor that varies between (0 - 10), the input voltage that varies between (100 V - 400 V), and to facilitate visualization on a graph of three dimensions, the ratio L_1/L_2 was kept fixed at 0.89. The graphic result of this variation is presented in Figure 5.

All points belonging to the three-dimensional planes illustrated in Figure 5 satisfy the design specifications, however, depending on the position of the point it is possible to obtain specific characteristics for the variables of interest (D, I_1, I_2, V_{C1} and V_{C2}). As an example, the black dot positioned in the graphs was chosen with the aim of obtaining maximum circuit efficiency. It can be seen that at this point in the design

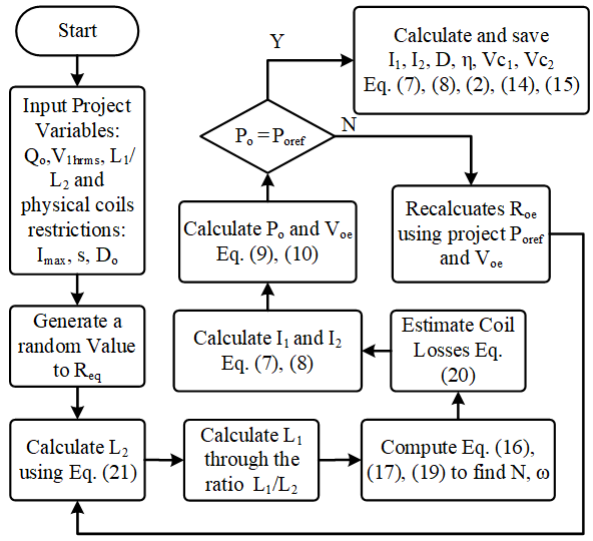

Figure 4: Block diagram of the interactive algorithm for IPT circuit simulation.

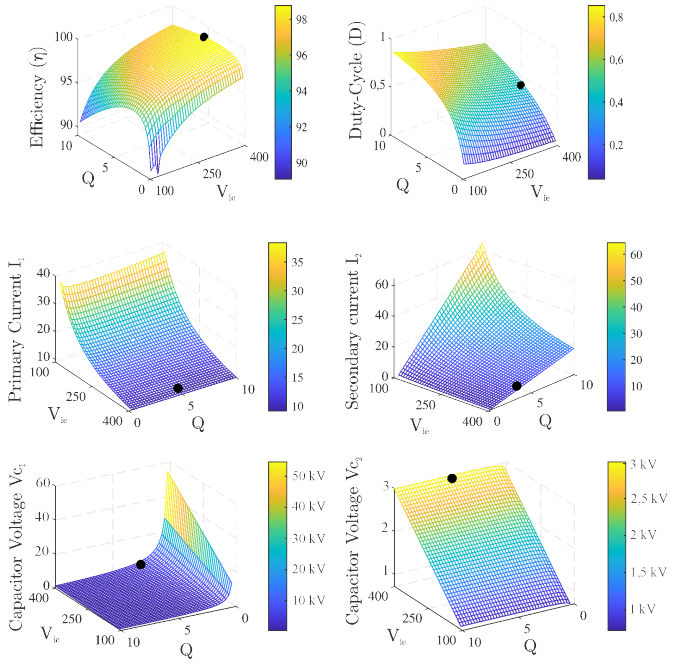

Figure 5: The variables (a) (η) , (b) D , (c) I_1 , (d) I_2 , (e) V_{C1} and (f) V_{C2} as a function of the variation of Q_o and V_{ie} keeping the ratio L_1/L_2 fixed at 0.89

.

the peak voltage in the capacitors reaches high values, which could be a problem with regard to the insulation of the circuit components. Furthermore, this voltage level is also reflected at the terminals of the transmission and reception coils, thus complicating their physical design. Therefore, it becomes interesting to develop a design method that guarantees maximum efficiency taking into account restrictions.

Table II: Project parameters obtained.

Parameter		**Value**
Primary inductance of the coil	L_1	120 μH
Secondary inductance of the coil	L_2	136 μH
Input voltage	V_{ie}	210 V
Duty-Cycle of Buck-Boost converter	D	0.577
compensation capacitor	C_1	29.11 nF
Secondary compensation capacitor	C_2	25.71 nF
Series resistance primary inductor	r_{L1}	128 mΩ
Series resistance secondary inductor	r_{L2}	137 mΩ
Output resistance	R_{oe}	15.68 Ω

C. Optimization design algorithm

The objective of the algorithm is to vary the designs variables to guarantee the design specifications, maximizing efficiency, which consists of reducing the series resistance of the coils (r_{L1}, r_{L2}), guaranteeing arbitrated maximum operating limits based on the available components. Through the elaboration of a optimization problem

$$J \rightarrow \{Max\ Eq.13\}$$
$$g \rightarrow \left\{ \begin{array}{l} I_1 < I_{1ref} \\ I_1 < I_{1ref} \\ Vc_1 < Vc_{1ref} \\ Vc_2 < Vc_{2ref} \\ D_{\min} < D < D_{\max} \end{array} \right\} \quad (22)$$

In this optimization problem, the aim is to maximize yield through the cost function J, taking into account the restrictions defined in g. The optimization method chosen to design the parameters was particle swarm optimization. The great advantage of using PSO is its easy implementation, using only primitive structures and mathematical operators without great computational cost [20].

The solutions in the PSO algorithm are called particles, they travel through an n-dimensional space, formed by the parameters to be varied. The particles move using the best positions found as a reference, where the best position is the one in which the objective function reaches the highest/minimum values. By executing the algorithm using the project specifications and de follow operating limits

- I_{1ref} and I_{2ref}: 20 A
- V_{C1} and V_{C2}: 1600 V
- V_{ie} max: 400 V
- D: 0.7>D>0.3
- D_o: 50 cm

Figure 6 illustrates the behavior of the particles for the first and last iteration of the algorithm. In Figure 6 the red square represents the position of the particle whose highest yield was obtained, respecting the established limits. It can be observed that throughout the interactions the particles concentrate around a zone that the algorithm interprets as having the best solutions to the problem. The Table II presents the design parameters found for the arbitrated specifications and restrictions.

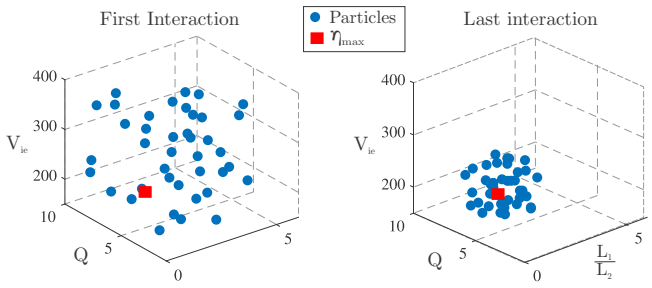

Figure 6: Position of particles in the plane (V_{ie}, L_1/L_2, Q) during the first (a) and last iteration (b) of the PSO algorithm.

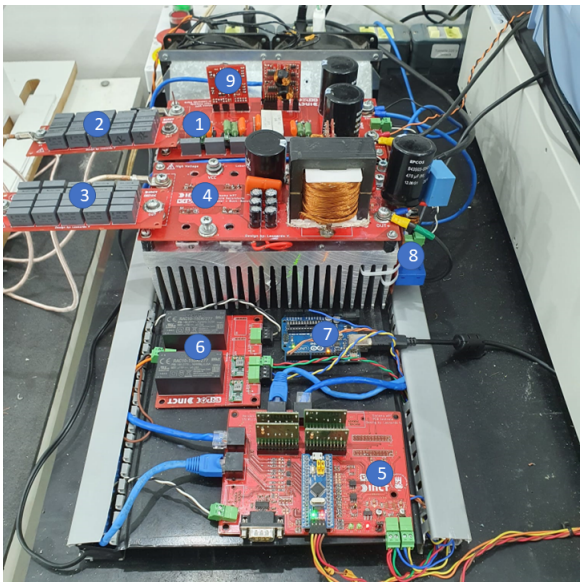

Figure 7: IPT Converter Experimental Platform.

IV. Experimental Validation

In order to validate the IPT converter design for applications in EV chargers, this section presents the experimental results obtained through the development of a prototype.

Figure 7 illustrates the practical assembly of the system. Considering that this is a prototype, it was decided to develop the system in a modular way, where the modules are numbered in Figure 7. Module 1 is the input full bridge inverter, module 2 is the primary compensation capacitors, module 3 the secondary compensation capacitors. Module 4 represents the rectifier bridge and the output buck-boost converter. Module 5 is the control and signal conditioning circuit. Module 6 is the auxiliary power circuit. Module 7 is the communication interface with the computer, module 8 is the instrumentation circuit and finally module 9 is the gate driver circuits.

Using the electrical parameters obtained through optimized design, physical execution of the transmission (Tx) and reception (Rx) coils were carried out, illustrated in Figure 8. It can be seen that the coils were installed on a platform that allows vertical and horizontal distance adjustment. For

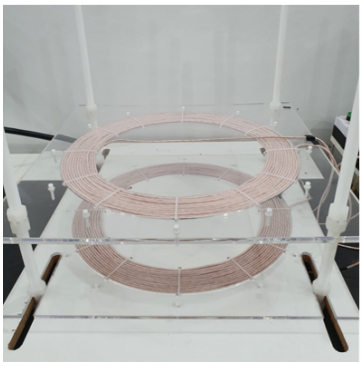

Figure 8: Transmission and receiving coils and their supporting platform.

Table III: Practical parametric features of coils.

Parameters	Tx Coil	Rx Coil	Unit
Inductance (L)	118.80	134.13	μH
Number of turns (N)	12.5	13.5	-
Inner diameter (D_i)	375	365	mm
Outer diameter (D_o)	500	500	mm
Wire length (l)	-	-	m
Equivalent resistance (Req)	-	-	mΩ
Mutual inductance (M)	23.76	27.09	μH
Coupling coefficient (k)	0.202	0.202	-

nominal system operation, the vertical distance is 16 cm and the horizontal misalignment is 0 cm.

Another feature of the coil platform is that its structure is entirely built with non-ferromagnetic materials, which contributes to more accurate measurements, where the induction of eddy currents can be minimized. The practical parameters of the coils are presented in Table III.

Through Figure 9 and Figure 10 it can be seen waveforms of currents and voltages in the resonant tanks of the IPT circuit. The blue waves represent the voltages on the compensation capacitors, the green waves the voltages on the coils and the pink waves the currents in the coils.

From Figure 9 and 10 it can be seen that the maximum

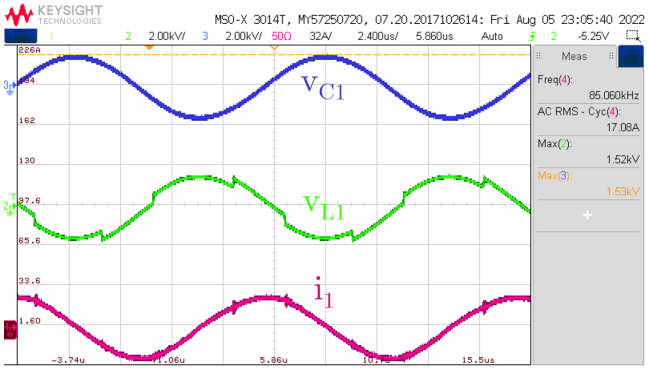

Figure 9: Waveforms of voltage in the primary capacitor (v_{C1}), voltage in the primary coil (v_{L1}) and primary current (i_1).

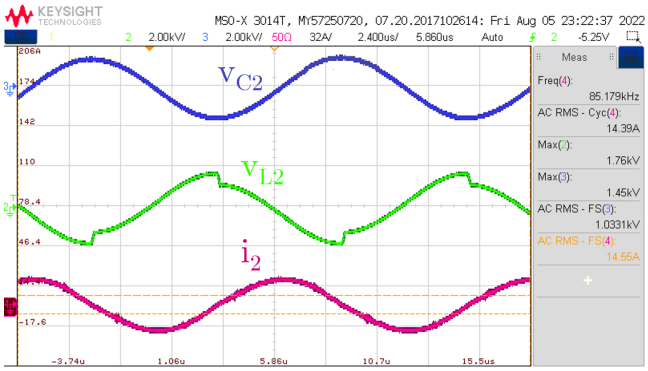

Figure 10: Waveforms of voltage in the secondary capacitor (v_{C2}), voltage in the secondary coil (v_{L2}) and secondary current (i_2).

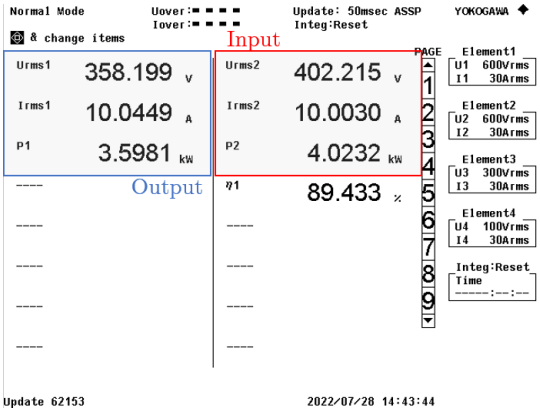

Figure 11: Input and output characteristics measured by Yokogawa WT3000E analyzer.

peak voltage in the compensation capacitors remained within the limits stipulated in the project, as well as the primary and secondary current.

A performance analysis was carried out with the Yokogawa WT3000E analyzer, where a total efficiency of 89.4 % was obtained for nominal operation as show Figure 11. Through the analyzer screen, it is possible to check the input voltage (U_{rms2}), input current (I_{rms2}) and input power P_2. And in the same way, the output voltage (U_{rms1}), output current (I_{rms1}) and output power P_2 are checked.

A performance analysis was carried out with the Yokogawa WT3000E analyzer, where a total efficiency of 89.4 % was obtained for nominal operation as show Figure 11. Through the analyzer screen, it is possible to check the input voltage (U_{rms2}), input current (I_{rms2}) and input power P_2. And in the same way, the output voltage (U_{rms1}), output current (I_{rms1}) and output power P_2 are checked.

V. Conclusion

IPT charging is a technology that can contribute to the development and consolidation of electric vehicles. However, it still has development limitations mainly linked to the design and efficiency in the wireless transfer process. The methodology proposed in this article makes it possible to optimize efficiency while ensuring system operation within established limits, which are linked to system isolation (voltage in coils and capacitors) and maximum currents in semiconductors. In this way, manufacturers can adapt the portfolio of components for the development of wireless chargers. The practical prototype presented adequate functioning, with the limitations satisfied and adequate performance taking into account the SAE-J295 standard.

Acknowledgment

This work was financed in part by the Coordination for the Improvement of Higher Education Personnel – Brazil (CAPES/PROEX) – Finance Code 001. I thank INCT-GD and the funding bodies (CNPq process 465640/2014-1, CAPES process no. 23038.000776/2017-54 and FAPERGS 17/2551-0000517-1) for the financial support.

References

[1] IEA, "World energy outlook 2021," international energy agency, https://www.iea.org/reports/world-energy-outlook-2021.,, Tech. Rep., 2021.

[2] A. Nordelöf, M. Messagie, A.-M. Tillman, M. Ljunggren, and J. Van Mierlo, "Environmental impacts of hybrid, plug-in hybrid, and battery electric vehicles—what can we learn from life cycle assessment?" *The International Journal of Life Cycle Assessment*, vol. 19, 08 2014.

[3] ABVE, "Eletrificados batem todas as previsões em 2021," ASSOCIAÇÃO BRASILEIRA DE VEÍCULOS ELETRICOS, https://www.abve.org.br/eletrificados-batem-todas-as-previsoes-em-2021/, acesso 05/2022, Tech. Rep., 2022.

[4] ANFAVEA, "anuário da indústria automobilística brasileira," Associação Nacional dos Fabricantes de Veículos Automotores, ¡https://anfavea.com.br/anuario2022/2022.pdf, acesso: 08/2022, Tech. Rep., 2022.

[5] X. Mou, O. Groling, A. Gallant, and H. Sun, "Energy efficient and adaptive design for wireless power transfer in electric vehicles," in *2016 IEEE 83rd Vehicular Technology Conference (VTC Spring)*, 2016, pp. 1–5.

[6] A. A. S. Mohamed, S. An, and O. Mohammed, "Coil design optimization of power pad in ipt system for electric vehicle applications," *IEEE Transactions on Magnetics*, vol. 54, no. 4, pp. 1–5, 2018.

[7] T. Duerbaum, "First harmonic approximation including design constraints," in *INTELEC - Twentieth International Telecommunications Energy Conference (Cat. No.98CH36263)*, 1998, pp. 321–328.

[8] A. K. Rathore and V. R. Vakacharla, "A simple technique for fundamental harmonic approximation analysis in parallel and series–parallel resonant converters," *IEEE Transactions on Industrial Electronics*, vol. 67, no. 11, pp. 9963–9968, 2020.

[9] W. Zhang and C. C. Mi, "Compensation topologies of high-power wireless power transfer systems," *IEEE Transactions on Vehicular Technology*, vol. 65, no. 6, pp. 4768–4778, 2016.

[10] M. Zamani, M. Nagrial, J. Rizk, and A. Hellany, "A review of inductive power transfer for electric vehicles," in *2019 International Conference on Electrical Engineering Research Practice (ICEERP)*, 2019, pp. 1–5.

[11] A. Alphones and P. Jayathurathnage, "Review on wireless power transfer technology (invited paper)," in *2017 IEEE Asia Pacific Microwave Conference (APMC)*, 2017, pp. 326–329.

[12] C. Nataraj, S. Khan, M. Habaebi, and A. Muthalif, "Analysis of mutual inductance and coupling factor of inductively coupled coils for wireless electricity," *ARPN Journal of Engineering and Applied Sciences*, vol. 12, pp. 4007–4012, 07 2017.

[13] A. Iyer, C. Bharatiraja, I. Vaghasia, and V. Rajesh, "Design optimisation for an efficient wireless power transfer system for electric vehicles," *Energy Procedia*, vol. 117, pp. 1015–1023, 06 2017.

[14] S. Mohan, M. del Mar Hershenson, S. Boyd, and T. Lee, "Simple accurate expressions for planar spiral inductances," *IEEE Journal of Solid-State Circuits*, vol. 34, no. 10, pp. 1419–1424, 1999.

[15] G. Buja, M. Bertoluzzo, and K. N. Mude, "Design and experimentation of wpt charger for electric city car," *IEEE Transactions on Industrial Electronics*, vol. 62, no. 12, pp. 7436–7447, 2015.

[16] H. Li, J. Li, K. Wang, W. Chen, and X. Yang, "A maximum efficiency point tracking control scheme for wireless power transfer systems using magnetic resonant coupling," *IEEE Transactions on Power Electronics*, vol. 30, no. 7, pp. 3998–4008, 2015.

[17] H. Movagharnejad and A. Mertens, "Design metrics of compensation methods for contactless charging of electric vehicles," in *2017 19th European Conference on Power Electronics and Applications (EPE'17 ECCE Europe)*, 2017, pp. P.1–P.10.

[18] R. Bosshard, J. W. Kolar, J. Mühlethaler, I. Stevanović, B. Wunsch, and F. Canales, "Modeling and η - α -pareto optimization of inductive power transfer coils for electric vehicles," *IEEE Journal of Emerging and Selected Topics in Power Electronics*, vol. 3, no. 1, pp. 50–64, 2015.

[19] K. Aditya and V. K. Sood, "Design of 3.3 kw wireless battery charger for electric vehicle application considering bifurcation," in *2017 IEEE Electrical Power and Energy Conference (EPEC)*, 2017, pp. 1–6.

[20] J. Kennedy and R. Eberhart, "Particle swarm optimization," in *Proceedings of ICNN'95 - International Conference on Neural Networks*, vol. 4, 1995, pp. 1942–1948 vol.4.